STMAC: Spatio-Temporal Coordination-Based MAC Protocol for Driving Safety in Urban Vehicular Networks

Jaehoon Jeong, *Member, IEEE*, Yiwen Shen, *Student Member, IEEE*, Sangsoo Jeong, *Student Member, IEEE*, Sejun Lee, *Student Member, IEEE*, Hwanseok Jeong, *Student Member, IEEE*, Tae Oh, *Senior Member, IEEE*, Taejoon Park, *Member, IEEE*, Muhammad Usman Ilyas, *Member, IEEE*, Sang Hyuk Son, *Fellow, IEEE*, and David H. C. Du, *Fellow, IEEE*

***Abstract*— In this paper, we propose a spatio-temporal coordination-based media access control (STMAC) protocol for efficiently sharing driving safety information in urban vehicular networks. STMAC exploits a unique spatio-temporal feature characterized from a geometric relation among vehicles to form a line-of-collision graph, which shows the relationship among vehicles that may collide with each other. Based on this graph, we propose a contention-free channel access scheme to exchange safety messages simultaneously by employing directional antenna and transmission power control. Based on an urban road layout, we propose an optimized contention period schedule by considering the arrival rate of vehicles at an intersection in the communication range of a road-side unit to reduce vehicle registration time. Using theoretical analysis and extensive simulations, it is shown that STMAC outperforms legacy MAC protocols especially in a traffic congestion scenario. In the congestion case, STMAC can reduce the average superframe duration by 66.7%, packet end-to-end delay by 68.3%, and packet loss ratio by 88% in comparison with the existing MAC protocol for vehicle-to-infrastructure communication, based on the IEEE 802.11p.**

***Index Terms*— Vehicular networks, spatio-temporal, safety, MAC protocol, coordination.**

I. Introduction

DRIVING safety is one of the most important issues since approximately 1.24 million people die each year globally as a result of traffic accidents. Vehicular ad hoc networks (VANETs) have been highlighted and implemented during the last decade to support wireless communications for driving safety in road networks [1], [2]. Driving safety can be improved by an assistance of rapid exchanged of driving information among neighboring vehicles. As an important trend, dedicated short-range communications (DSRC) [3] were standardized as IEEE 802.11p in 2010 (now incorporated into IEEE 802.11 protocol [4]) for wireless access in vehicular environments (WAVE) [2], [5]. IEEE WAVE protocol is a multi-channel MAC protocol [4], adopting the enhanced distributed channel access (EDCA) [5] for quality of service (QoS) in vehicular environments. Many research results [6]–[9] show that a performance of WAVE deteriorates when a density of vehicles is high, approaching the performance of a slotted ALOHA process [8]. As a result, many MAC protocols [10]–[16] have been proposed to improve the performance of WAVE. However, the MAC protocols were not designed to support the geometric relation among vehicles for the driving safety and didn't consider the operation in an urban road environment.

A MAC protocol can operate in a distributed coordination function (DCF) mode (i.e., contention based), a point coordination function (PCF) mode (*i.e.*, contention-free based) or a hybrid coordination function (HCF) mode [4]. For driving safety in vehicular environments, a MAC protocol in the DCF-mode executes based on carrier sense multiple access with collision avoidance (CSMA/CA) [4] mechanism. This distributed approach can incur high frame collision rates at congested intersections in an urban environment [6]–[9], and in a scenario of a lack of comprehensive vehicle traffic. As a result, it may lead to an unreliable, non-prompt data exchange. On the contrary, a MAC protocol in the PCF-mode can wield road-side units (RSUs) or access points (APs) as coordinators to

Manuscript received September 19, 2016; revised March 4, 2017 and May 24, 2017; accepted July 2, 2017. Date of publication August 23, 2017; date of current version May 2, 2018. This work was supported in part by the Basic Science Research Program through the National Research Foundation of Korea (NRF) funded by the Ministry of Science, ICT & Future Planning (MSIP) under Grant 2014R1A1A1006438, in part by the Ministry of Education under Grant 2017R1D1A1B03035885, and in part by the Global Research Laboratory Program through the NRF and the DGIST Research and Development Program (CPS Global Center) funded by the MSIP under Grant 2013K1A1A2A02078326. The Associate Editor for this paper was L. Li. *(Corresponding author: Sang Hyuk Son.)*

J. Jeong is with the Department of Interaction Science, Sungkyunkwan University, Suwon 16419, South Korea (e-mail: pauljeong@skku.edu).

Y. Shen and H. Jeong are with the Department of Computer Science & Engineering, Sungkyunkwan University, Suwon 16419, South Korea (e-mail: chrisshen@skku.edu; harryjeong@skku.edu).

S. Lee is with the Korea Electronics Technology Institute, Seongnam-si 13509, South Korea (e-mail: sejunlee@skku.edu).

S. Jeong and S. H. Son are with the Department of Information and Communication Engineering, DGIST, Daegu 42988, South Korea (e-mail: 88jeongss@dgist.ac.kr; son@dgist.ac.kr).

T. Oh is with the Department of Information Sciences & Technologies, Rochester Institute of Technology, Rochester, NY 14623-5603 USA (e-mail: tom.oh@rit.edu).

T. Park is with the Department of Robotics Engineering, Hanyang University, Ansan 15588, South Korea (e-mail: taejoon@hanyang.ac.kr).

M. U. Ilyas is with the Department of Electrical Engineering, National University of Sciences and Technology, Islamabad 44000, Pakistan, and also with the Department of Computer Science, Faculty of Computing and Information Technology, University of Jeddah, Jeddah 21589, Saudi Arabia (e-mail: usman.ilyas@seecs.edu.pk; milyas@uj.edu.sa).

D. H. C. Du is with the Department of Computer Science & Engineering, University of Minnesota, Minneapolis, MN 55455 USA (e-mail: du@cs.umn.edu).

Color versions of one or more of the figures in this paper are available online at http://ieeexplore.ieee.org.

Digital Object Identifier 10.1109/TITS.2017.2723946

1524-9050 © 2017 IEEE. Personal use is permitted, but republication/redistribution requires IEEE permission.
See http://www.ieee.org/publications_standards/publications/rights/index.html for more information.

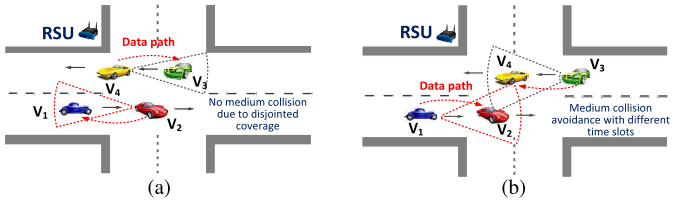

Fig. 1. Spatial and temporal coordination. (a) Spatial coordination. (b) Temporal coordination.

schedule time slots for transmitters. This centralized approach can reduce frame collision rates and guarantees a certain delay bound. However, this approach increases a data delivery delay since multiple transmitters must be managed. The HCF mode, which is a part of IEEE 802.11 [4], combines the PCF and DCF modes with QoS enhancement feature to deliver QoS data from vehicles to an RSU (i.e., AP). The HCF mode employs the HCF controlled channel access (HCCA) [4] as the PCF-mode for contention-free transfer, and the EDCA mechanism [4] as the DCF-mode for contention-based transfer. However, tailoring the optimal combination of the PCF and DCF modes still remains challenging research issues for the driving safety in vehicular environment.

On the other hand, for efficient communication among vehicles, RSUs are expected to be deployed at intersections and streets in vehicular networks [17]. RSUs with powerful computation capabilities can operate as edge devices [18] to coordinate channel access for vehicles while preventing channel collision and provides Internet connectivity to disseminate safety information. Thus, a cost for RSU implementation can be easily justified by the reduction of human injuries and deaths as well as property loss caused by road accidents. Also, an implementation of global positioning system (GPS) is another important trend in vehicular networks. Navigators (*i.e.*, a dedicated GPS navigator [19] and a smartphone navigation app [20]) are commonly used by drivers who are driving to destinations in unfamiliar areas. An RSU can collect GPS data of vehicles in its area so that the transmission schedule of vehicles can be optimized. Therefore, RSUs can be used as coordinators to orchestrate communications among vehicles. However, few studies have explored the important functions of RSUs for driving safety.

In this paper, we propose a Spatio-Temporal coordination based MAC (STMAC) protocol for urban scenarios, utilizing a spatio-temporal feature and a road layout feature in urban areas for better wireless channel access in vehicular networks. The objective of STMAC is to support reliable and fast data exchange among vehicles for driving safety via the coordination of vehicular infrastructure, such as RSUs. STMAC leverages a unique spatio-temporal feature to form a line-of-collision (LoC) graph in which multiple vehicles can transmit in the same time slot without channel interferences or collisions by utilizing directional antennas and transmission power control. As shown in Fig. 1(a), the spatial disjoint of communication areas enabled by directional antennas provides the feature of spatial reuse, whereas the overlap of the communication areas shown in Fig. 1(b) indicates a temporal feature by which the communications should be separated for collision avoidance. Further, based on the urban road layout, we propose a scheme that optimizes the contention period for vehicle registration into an RSU by reducing the contention duration by considering the vehicle arrival rate at an intersection. Our STMAC can facilitate the rapid exchange of driving information among neighboring vehicles. This rapid exchange can help drivers to get driving assistance information for avoiding possible collisions. Even in self-driving, STMAC can help autonomous vehicles avoid collision by exchanging the mobility information and cooperating with each other for driving coordination.

The contributions of this paper are as follows:

- **An LoC graph based channel access scheme via an enhanced set-cover algorithm is proposed:** STMAC's set-cover algorithm handles an *unfixed* subset family of elements where each subset is covered by a time slot, and each element is a transmission, which differs from the legacy set-cover algorithm [21] handling a *fixed* subset family of elements. This algorithm schedules multiple vehicles to transmit their safety messages simultaneously in spatially disjointed transmission areas (see Section IV-A).
- **A contention period optimization is proposed for the efficient channel usage:** STMAC's contention period adapts the vehicle arrival rate at an intersection in an urban area for better channel utilization. This optimization is feasible in vehicular networks where vehicles move along confined roadways (see Section IV-B).
- **A new hybrid MAC protocol is proposed using spatio-temporal coordination:** STMAC uses the PCF mode to register vehicles for a time slot allocation as well as an emergency message dissemination from an RSU to vehicles. It uses the DCF mode for both safety message exchange and emergency message dissemination among vehicles by *spatio-temporal coordination*. (see Section V).

Through theoretical analysis and extensive simulations, it is shown that STMAC outperforms other state-of-the-art protocols in terms of average superframe duration, end-to-end (E2E) delay, and packet loss ratio.

The remainder of this paper is organized as follows. In Section II, related work is summarized along with analysis. Section III discusses the assumptions and scenarios used for problem formulation. Section IV describes the characterization of spatial-temporal features and the optimization of the contention period. In Section V, the STMAC protocol is proposed. In Section VI, we evaluate STMAC by comparing with baseline MAC protocols (*i.e.*, PCF and DCF MAC protocols) through theoretical data and simulation results. Finally, Section VII concludes this paper along with future work.

II. Related Work

IEEE 802.11 [4] defines an HCF-mode to use a contention-based channel access method for contention-based transfer called EDCA, and a controlled channel access for contention-free transfer called HCCA [4]. In contention-free transfer,

the HCCA mechanism [4] enables the stations to transmit their QoS data to the AP according to the schedule made by the AP without any contention. On the other hand, the stations attempt to transmit their prioritized QoS data to the AP with the EDCA mechanism [4]. In both modes, the station transmits its data to its neighboring station under its communication coverage via the AP. However, for the purpose of driving safety, direct data delivery is possible through vehicle-to-vehicle (V2V) communication without using the data relay of an RSU. Thus, we need to design a new hybrid mode for a reliable and fast data delivery among vehicles.

Many other MAC protocols have been proposed, using MAC coordination functions (*i.e.*, DCF and PCF) to improve the efficiency and reliability of wireless media access in mobile ad hoc networks (MANET) and vehicular ad hoc networks (VANET). In most cases, omni-directional antenna is considered for MAC protocols even though directional antenna has several benefits. Therefore, the literature review of MAC protocols is discussed according to the coordination functions along with antenna types.

Ko *et al.* [12] propose a directional antenna MAC protocol (D-MAC) in DCF. For concurrent communications and based on D-MAC, Feng et al. propose a location- and mobility-aware (LMA) MAC protocol [10]. Both D-MAC and LMA perform communications in DCF mode utilizing CSMA/CA and the exponential backoff mechanism for ad hoc networks. LMA is designed to achieve efficient V2V communication without infrastructure nodes (*e.g.*, RSU). The aim of LMA is to achieve efficient directional transmission while resolving the deafness problem [10]. Vehicles in LMA use the predicted location and mobility information of the target vehicle, thereby performing directed transmissions using beamforming. As an enhanced D-MAC protocol, LMA exploits the advantages of a directional antenna, such as spatial reuse, by considering the moving direction of a vehicle, and uses a longer transmission range in transmitting request-to-send (RTS), clear-to-send (CTS), data frame (DATA), and acknowledgment (ACK) as directed transmissions. However, the frame collisions increase substantially when both D-MAC and LMS are used when the vehicle density is high. This may result in a serious packet delivery delay, which is not acceptable for driving safety.

In PCF, Chung et al. propose a WAVE PCF MAC protocol (WPCF) [11] to improve the channel utilization and user capacity in vehicle-to-infrastructure (V2I) or infrastructure-to-vehicle (I2V) communication. The main purpose of WPCF is to provide multiple vehicles with time-coordinated wireless media access for the efficient communication with an RSU. As a result, WPCF can increase the channel efficiency when multiple vehicles attempt to sequentially communicate with an RSU [17]. WPCF also suggests a handover mechanism by adopting a WAVE handover controller to minimize service disconnection time [11]. However, since WPCF neither optimizes the length of a contention period (CP) nor utilizes concurrent transmissions in a contention-free period (CFP), the utilization of the wireless channel still needs to be improved. Unlike WPCF, which is a kind of HCF, STMAC allows vehicles to exchange their driving information with their neighboring vehicles without the relaying of an RSU. Note that since WPCF is an Infrastructure-to-Vehicle (I2V) MAC protocol, the Vehicle-to-Vehicle (V2V) data delivery requires the relay via an RSU. Because this exchange is performed concurrently for the disjoint sets of vehicles, the packet delivery delay of STMAC is shorter than that of WPCF. Kim et al. propose a MAC protocol using a road traffic estimation for I2V communication in a highway environment [22]. Their MAC protocol estimates the road traffic to precisely control the transmission probability of vehicles in order to maximize system throughput. The protocol also presents a mechanism to use a threshold to limit the number of transmitted packets for fairness among vehicles. Hafeez et al. propose a distributed multichannel and mobility-aware cluster-based MAC protocol, called DMMAC [14]. DMMAC utilizes the EDCA of IEEE 802.11p to differentiate the types of packets, enables vehicles to form clusters based on a weighted stabilization factor to exchange packets.

Through the evaluation of the existing MAC protocols, we found that LMA, WPCF, and DMMAC are representatives of DCF, PCF, and cluster-based MAC protocols in VANET, respectively. Hence, the three protocols are used as baselines for performance evaluation in this paper. Comparing with LMA, WPCF, and DMMAC, STMAC leverages a spatio-temporal feature to improve the efficiency of channel access and reduce the delivery delay of safety messages. STMAC also considers an urban layout to reduce the length of the contention period. Therefore, the results will show that STMAC can outperform the legacy MAC protocols, such as LMA, WPCF, and DMMAC.

III. Problem Formulation

The goal of the STMAC protocol is to provide a reliable and fast message exchange among adjacent vehicles through the coordination of an RSU for safe driving. To achieve this goal, a directed transmission is used whenever possible to maximize the number of concurrent transmissions through spatio-temporal transmission scheduling. In the following section, we specify several assumptions and a target scenario.

A. Assumptions

The following assumptions are made in the course of designing STMAC:

- Vehicles are equipped with a DSRC interface [2] and a directional antenna array with the phase shifting [10], [23], whereas RSUs are equipped with an omnidirectional antenna. The directional antenna array can generate multiple beams toward multiple receivers at the same time (*e.g.*, MU-MIMO) [24], [25]. The narrow beam problem can be avoided in our STMAC. The direction of each beam and the communication coverage (*i.e.*, R and β, where R is the communication range defined as a distance where a successful data frame from a sender vehicle can be transmitted to a receiver vehicle with almost no bit error, and β is the communication beam angle that is constructed by the

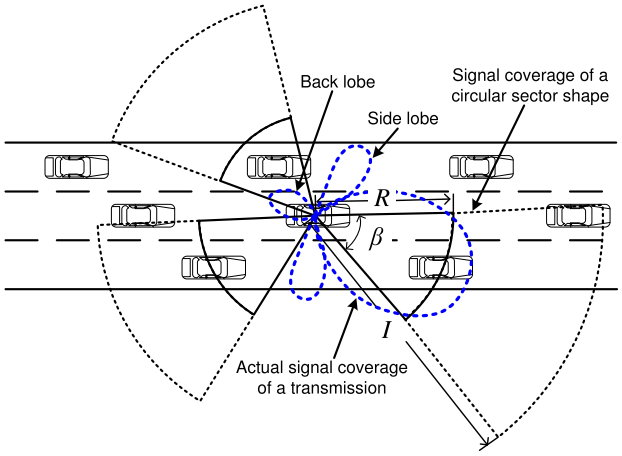

Fig. 2. A transmission signal coverage and interference range.

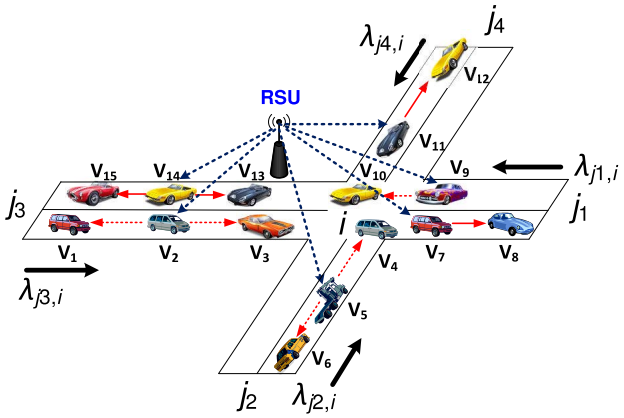

Fig. 3. The target scenario of spatio-temporal coordination by the RSU.

phase shifting of the directional antenna array [23]) are adjustable by locating the receiving vehicle's location and controlling RF transmission power [10], [23], [26], as shown in Fig. 2. The RF transmission power W_t can be determined as follows:

$$W_t = \frac{(2d)^{\alpha} \cdot (4\pi)^2 \cdot W_r}{\Lambda^2}, \tag{1}$$

where d is the distance between a transmitter and a receiver; α is the minimum path loss coefficient; Λ is the wavelength of a signal; W_r is the minimum power level to be able to physically receive a signal, which can be calculated by $W_r = 10^{sa/10}$, and sa is the minimum signal attenuation threshold.

- For simplicity, the interference range I of a transmission is considered to be two times the communication range R, as shown in Fig. 2, which is used in an algorithm (Algorithm 1 in Section IV-A) to decide an interference set when calculating a transmission schedule. Also, as shown in Fig. 2, a circular-sector-shape signal coverage is considered instead of the actual transmission signal coverage, and the side lobes and the back lobe are ignored for the simplicity of modeling.
- A procedure of handover similar to that of WPCF [11] is implemented in this work by using two DSRC service channels [2]. The first channel is used for the RSU's coverage, and the second channel is used for the adjacent RSU's coverage. The detailed description of the handover is given in WPCF [11].
- Vehicles are equipped with a GPS-based navigation system [19], [20]. This GPS navigation system provides vehicles with their position, speed, and direction at any time.
- The effect of buildings or trees (called terrain effect) exists in real vehicular networks. The Nakagami fading model [27] is usually used for vehicular networks. If a better fading model considering terrain effect is available, our STMAC protocol can accommodate such a model.

B. Target Scenario

Our target scenario is a vehicle data exchange, such as mobility information (*e.g.*, location, direction, and speed) and in-vehicle device status (*e.g.*, break, gear, engine, and axle), for driving safety in urban road networks. As shown in Fig. 3, RSUs are typically deployed at road intersections and serve as gateways between VANET and the intelligent transportation systems (ITS) infrastructure [17]. An RSU's transmission coverage range is set to cover the maximum of the lengths of the halves of the road segments. The inter-RSU interference is avoided by letting two adjacent RSUs use different DSRC service channels. Vehicles periodically transmit time slot requests to an RSU along with their mobility information (*i.e.*, current location, moving direction, and speed). The RSU uses the request information to construct a transmission schedule for the wireless channel access. Using the assigned time slots from the schedule, safety messages are directly exchanged between neighbor vehicles to prevent accidents. In the next section, we will explain the spatio-temporal feature and contention period optimization in STMAC protocol.

IV. Spatio-Temporal Coordination and Contention Period Optimization

In this section, we propose a new channel access scheme based on an enhanced set-cover algorithm by characterizing a spatio-temporal feature in urban vehicular networks. We also propose a contention period adaptation based on the vehicle arrival rate at an intersection in an urban area. To characterize the spatio-temporal feature in a vehicular environment, the formation of the line-of-collision (LoC) graph is first explained.

A. Spatio-Temporal Coordination Based Channel Access

In an urban area, a vehicle accident is usually a direct crash or collision among vehicles (*e.g.*, frontal, side, and rear impacts). Preventing the initial direct crash can largely reduce fatalities and property losses. We propose an LoC graph among vehicles based on a geometric relation to describe the initial direct crash. As shown in Fig. 4, vehicles A and B have an LoC relation because there are no middle vehicles between them, and can therefore crash directly. From A, two tangent

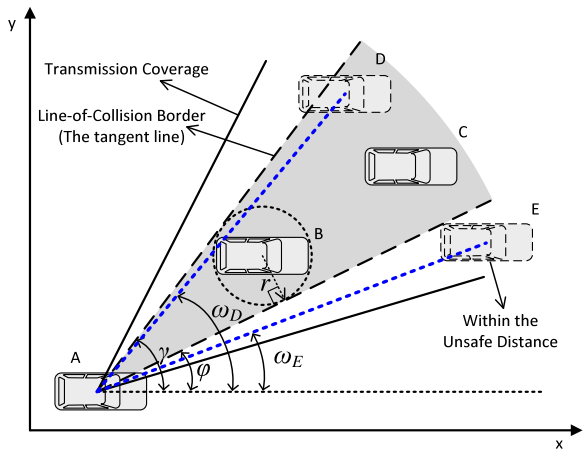

Fig. 4. Line-of-collision relation construction.

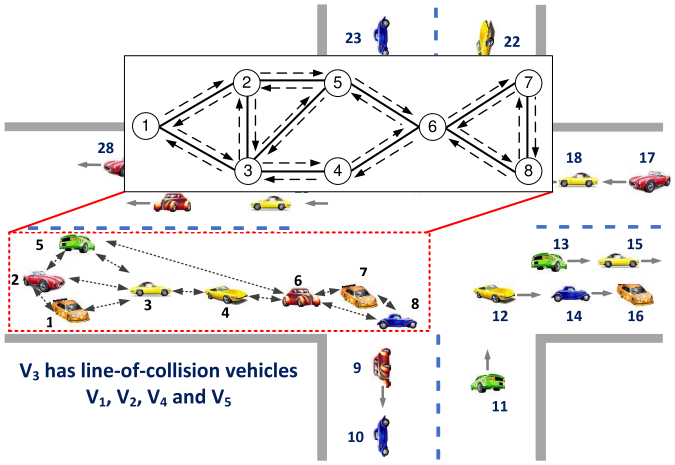

Fig. 5. Line-of-collision vehicles in road segment with multiple lanes.

lines on a circle can be derived based on the half length (as a radius r) of B. Any vehicle within the area between the two tangent lines (gray area in Fig. 4), but farther than B, is considered as a non-LoC vehicle to A, *e.g.*, C in Fig. 4. By comparing the two angles γ and φ of the two tangent lines and the unsafe distance determined by the two-second rule [28], it can also be determined whether or not any other vehicles can be LoC vehicles of A. For example, D has no LoC relation with A because the angle ω_D is smaller than γ, but larger than φ. On the other hand, E is an LoC vehicle of A, based on the fact that the angle ω_E is smaller than φ and is within the unsafe distance. Note that vehicles with different sizes can be considered as the same class, *e.g.*, a vehicle with a length smaller than 5 meters can be categorized as a 5 meter vehicle to determine the radius r. From communication collision point of view, if C is in the interference range of A, which is 2 times transmission range of A [29], C can be interfered. But in Algorithm 1, this interference is avoided by scheduling vehicles A and C in different time slots, which means if C is in the interference range of A, when A is transmitting to B, C will neither receiving nor sending a packet. Note that LoC means Line of Collision, which indicates the relationship of directly physically collision of two neighboring vehicles rather than the line-of-sight for communication range.

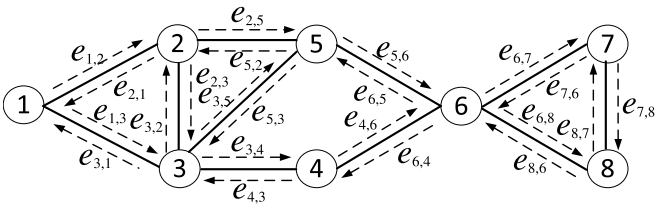

Start node	Edges in a time slot
3, 7	$S_1 = \{e_{3,1}, e_{3,2}, e_{3,4}, e_{3,5}, e_{7,6}, e_{7,8}\}$
2, 8	$S_2 = \{e_{2,1}, e_{2,3}, e_{2,5}, e_{8,6}, e_{8,7}\}$
1, 6	$S_3 = \{e_{1,2}, e_{1,3}, e_{6,4}, e_{6,5}, e_{6,7}, e_{6,8}\}$
5	$S_4 = \{e_{5,2}, e_{5,3}, e_{5,6}\}$
4	$S_5 = \{e_{4,3}, e_{4,6}\}$

Fig. 6. Searching sequence for maximum compatible cover-sets.

Based on the LoC relation, an LoC graph can be constructed. As shown in the dotted box of Fig. 5, we consider a scenario in which vehicles are moving in multiple lanes in road segments. The solid box in Fig. 5 shows an LoC graph $G = (V, E)$ constructed by the vehicles inside the dotted box, where the vertices in V are vehicles and the edges in E indicate an LoC relation between two adjacent vehicles that can collide directly with each other. Thus, the continuous communications are necessary for the connected vehicles in the LoC graph G. Notice that the LoC graph is used in our STMAC protocol to reduce medium collision, which is discussed in later in this section.

Through the LoC graph of the vehicles, we propose a spatio-temporal coordination based channel access scheme by using an enhanced set-cover algorithm. The enhanced set-cover algorithm for STMAC attempts to find a minimum set-cover for an optimal time slot allocation in a given LoC graph. Our *STMAC Set-Cover algorithm* attempts to *allow as many concurrent transmissions as possible in each time slot in order to reduce the contention-free period for the required transmissions of all the LoC vehicles*.

We define the following terms for the STMAC Set-Cover algorithm:

Definition 1 (Cover-Set): Let ***Cover-Set*** *be a set S_i of edges in an LoC graph G where the edges are* ***mutually not interfering*** *(i.e.,* ***compatible****) with each other, that is, any pair of edges $e_{u,v}, e_{x,y} \in E(G)$ are compatible with each other. For example, as shown in Fig. 6, the cover-set S_1 is $\{e_{3,1}, e_{3,2}, e_{3,4}, e_{3,5}, e_{7,6}, e_{7,8}\}$ for time slot* 1.

Definition 2 (Set-Cover): Let ***Set-Cover*** *be a set S of cover-sets S_i for $i = 1 \cdots n$ that is equal to the edge set $E(G)$ such that $E(G) = \bigcup_{i=1}^{n} S_i$. That is, the set-cover S includes all the directed edges in an LoC graph G and represents the schedule of concurrent transmissions of the edges in S_i for time slot i. For example, Fig. 6 shows the mapping between time slot i and cover-set S_i.*

We now formulate an optimization of a time slot allocation for cover-sets of non-interfering edges that can be transmitted concurrently. Let 2^N be a power set of natural number set N as time slot sets, such as $2^N = \{\emptyset, \{1\}, \{1, 2\}, \{1, 2, 3\}, ...\}$. Let S be a set-cover for a time slot schedule. Let E be a directed edge set. Let S_i be a cover-set for a time slot i. Let $E(S_i)$

be the set of non-interfering edges in S_i. The optimization of time slot allocation is as follows:

$$S^* \leftarrow \arg\min_{S \in 2^N} |S|, \tag{2}$$

where $S = \{S_i | S_i$ is a cover-set for time slot $i\}$ and $E = \bigcup_{S_i \in S} E(S_i)$.

For this optimization, we propose an STMAC Set-Cover algorithm as shown in Algorithm 1. The optimization objective of the STMAC Set-Cover algorithm is *to find a set-cover with the minimum number of time slots, mapped to cover-sets.* A schedule of cover-sets of which the edges are the concurrent transmissions for a specific time slot can be represented as a mapping from the set S of time slots S_i (*i.e.*, cover-sets) to edges $e_j \in E$. A set-cover returned as S by Algorithm 1 might not be optimal since the set-covering problem is originally NP-hard. That is, STMAC Set-Cover is an extension of the legacy Set-Cover [21], where families (*i.e.*, sets of elements) are fixed. However, in our STMAC Set-Cover, the families are not given, but should be dynamically constructed as cover-sets during the mapping. Each cover-set S_i needs a time slot i, so one time slot is mapped to a cover-set that is a set of non-interfering edges in G.

The lines 5-10 in Algorithm 1 show that the search for a new maximum cover-set, which is a cover-set with the maximum number of edges covered by a time slot, is repeated until all the edges in E are covered by cover-sets. Refer to Appendix B for the detailed description of $Search_Max_Compatible_Cover_Set(G, E')$ in line 6. The time complexity of Algorithm 1 is $O(E \cdot V \cdot (V + E))$. Since the number of vehicles at one intersection is still within a reasonable bound, the time taken to calculate the optimal cover set shall also be within a reasonable bound. The polynomial time complexity of Algorithm 1 can be efficiently handled by the edge-centric computing [18] in RSU.

Algorithm 1 STMAC-Set-Cover Algorithm

```
1: function STMAC_SET_COVER(G)          ▷ G is a line-of-collision (LoC) graph
2:     E' ← G(E) ▷ E' is the set of the remaining edges not belonging to any cover-set
3:     S ← ∅                            ▷ S is for a Set-Cover
4:     i ← 1
5:     while E' ≠ ∅ do
6:     S_i ← Search_Max_Compatible_Cover_Set(G, E')
         ▷ search for a Maximum Cover-Set for the remaining edges in E'
7:       E' ← E' − S_i
8:       S ← S ∪ {S_i}
9:       i ← i + 1
10:    end while
11:    return S
12: end function
```

Fig. 6 shows an example of a search sequence for a set-cover with maximum cover-sets by Algorithm 1. For the first time slot, in Fig. 6, vertex 3 is selected as a start node for time slot 1 because it has the highest degree. Vertex 7 can also transmit in time slot 1 since vertex 7 is not the receiver of vertex 3 and has a spatial disjoint feature. Next, vertexes 2 and 8 are selected as the next transmitters. Through a similar procedure for the remaining vehicles, 5 time slots can cover all the transmissions for the LoC graph G instead of 8 time slots for each vehicle. Thus, the mapping between time slot and cover-set is constructed by the STMAC Set-Cover algorithm for the transmission schedule.

Note that the STMAC Set-Cover algorithm can be extended to consider an interference range existing in real radio communications [29]. Algorithm 3 in Appendix B describes for the STMAC Set-Cover considering the interference range.

B. Contention Period Optimization

In this section, we explain the contention period optimization for the efficient channel usage, considering the arrival rate of unregistered vehicles to the communication range of an RSU at an intersection. This adaptation is possible because vehicles in an urban area move along the confined roadways, so the arrival rate can be measured in vehicular networks while such a measurement is not feasible in mobile ad hoc networks due to free mobility. Note that the arrival rate can be measured by several ways for object recognition, such as loop detectors and traffic cameras, which are installed at intersections.

The contention period is dynamically adapted according to the arrival rate of unregistered vehicles to the communication range of an RSU. As the number of vehicles increases for an RSU, the length of CFP in the superframe duration will increase, since more vehicles should be allocated with their time slots for channel access. Thus, the length of CP should be determined according to the expected number of arriving, unregistered vehicles in one superframe duration to enable the vehicles the opportunity to be registered in the RSU with a registration frame. If the CP length is too short, registration frames toward the RSU will encounter many collisions during registration attempts, and only a few vehicles can therefore be registered. In contrast, if the CP length is too long, most of the time in CP will be wasted after registering all arriving vehicles in the RSU, resulting in a poor channel utilization. Thus, we need to find the appropriate length of CP to guarantee that new incoming vehicles are given the opportunity to registered with the RSU in a finite period of time (*e.g.*, one superframe duration) within the same superframe.

Let $\lambda_{j_k i}$ denote the vehicle arrival rate from an adjacent intersection j_k to an intersection i, as shown in Fig. 3. Let λ be the total arrival rate for the communication range of RSU at intersection i per unit time (*e.g.*, 1 second) such that

$$\lambda = \sum_{k=1}^{n} \lambda_{j_k i}. \tag{3}$$

Here n is the number of neighbor intersections of intersection i. RSU at an intersection i observes the number of vehicles that arrive within its transmission coverage from its adjacent road segments. We can simply calculate λ with the total arrivals of vehicles for all incoming road segments per unit time.

We leverage the concept of the slotted ALOHA [30] and the Reservation-ALOHA (R-ALOHA) [31] for CP adaptation. The original R-ALOHA was designed for ad hoc networks to reduce collisions [32], whereas the CP in our scheme is designed for vehicle registration to reserve time slots in the next CFP. R-ALOHA provides nodes with time-based multiple channel access in a wireless link with a reasonable access efficiency (i.e., channel utilization) [31]. In CP, since new comer vehicles to an intersection area try to register their mobility information into the RSU with a single registration frame, R-ALOHA can be used for the CP in STMAC. Let s be the time duration of one superframe duration including CP and CFP duration.

- An unregistered vehicle attempts to send its registration frame with probability p.
- N vehicles attempt to be registered in RSU in this superframe duration, such that $N = \lambda \cdot s$.
- The probability that one vehicle succeeds in registering its transmission request for a slot among N vehicles is:

$$g_N = N \cdot p \cdot (1-p)^{N-1}. \tag{4}$$

For the CP duration, the total number of slots to register N vehicles is:

$$M = \sum_{i=N}^{1} \frac{1}{g_i} = \sum_{i=N}^{1} \frac{1}{i \cdot p \cdot (1-p)^{i-1}}. \tag{5}$$

Appendix A provides the detailed derivation for this equation.

For the efficient operation, the possible values of λ are mapped into a pair of the optimal channel access probability p and total slot number M in off-line processing. This pair of p and M for the current λ is announced to unregistered vehicles by an RSU through a timing advertisement frame (TAF), specified in Section V. Note that although the RSUs are responsible for the vehicle registration and the cover-set calculations, they can handle these procedures because each RSU only manages one intersection at which the number of vehicles is still bounded to a reasonable level, even in rush-hours.

So far, we have described the proposed spatio-temporal coordination-based channel access scheme and the contention period optimization. In the next section, we will introduce a new hybrid MAC protocol to combine the merits of PCF and DCF modes based on the proposed channel access scheme and the contention period optimization.

V. Spatio-Temporal Coordination Based Media Access Control Protocol

STMAC is a hybrid MAC protocol that combines the PCF and DCF modes for efficient channel utilization and quick driving safety information exchange. The PCF mode is used to (i) register unregistered vehicles in an RSU with their mobility information, (ii) construct a collision-free channel access schedule for registered vehicles, and (iii) announce the channel access schedule for V2V communications in a similar way to that of WPCF [11]. In contrast, the DCF mode is used to enable the safety messages of the registered vehicles to be exchanged with other registered vehicles and without frame collision in V2V communications.

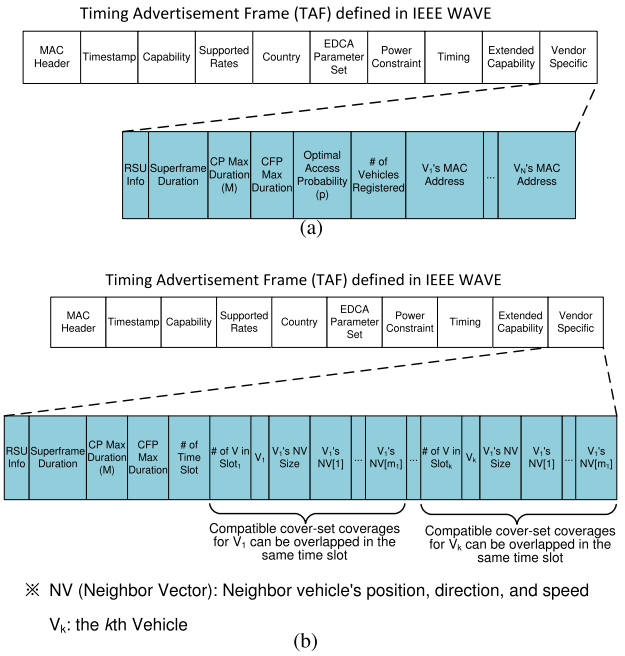

Fig. 7. Timing advertisement frame (TAF) formats in STMAC. (a) TAF in CP. (b) TAF in CFP.

In STMAC, an RSU periodically broadcasts a timing advertisement frame (TAF). The TAF is a beacon frame following the standard of the IEEE WAVE [4], [5]. In STMAC, it has two formats, including TAF in CP and TAF in CFP as shown in Fig. 7. Both formats in the vendor specific field have some common fields, such as RSU information, superframe duration, CP max duration (*i.e.*, M), and CFP max duration. The vendor specific field of TAF for CP shown in Fig. 7(a) additionally contains optimal access probability (*i.e.*, p), the number of vehicles registered, and registered vehicles' MAC addresses. The vendor specific field of TAF for CFP in Fig. 7(b) contains other information, such as the number of time slots, the transmission schedule in each time slot, and the neighbor vectors (NV). NV contains the mobility information (*i.e.*, the current position, direction, and speed) of neighboring vehicles.

In STMAC, time is divided into superframe duration, and each superframe duration consists of two phases, the CP phase and CFP phase, as shown in Fig. 8. These two phases are explained in the following subsections.

A. CP Phase for Vehicle Registration

In the CP phase, unregistered vehicles attempt to be registered in an RSU based on contention. Fig. 8(a) shows a contention-period time sequence for vehicle registration. As shown in Fig. 8(a), a TAF at the beginning of a CP is firstly transmitted by an RSU in a DSRC control channel (CCH), after a DCF interframe space (DIFS) period, indicating the start of a contention period.

The TAF mainly contains a list of the registered vehicles and the RSU's service channel number (SCH#) in the RSU Info part as shown in Fig. 7(a). Next, after receiving the TAF, the vehicles start contending the transmission opportunity to send a registration request (*i.e.*, REQ in Fig. 8(a)). It is possible

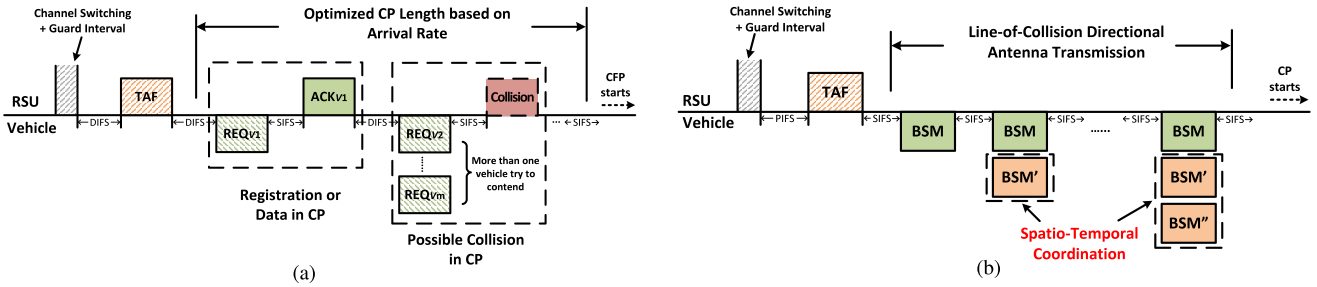

Fig. 8. Time sequence in STMAC protocol. (a) Contention-period time sequence. (b) Contention-free-period time sequence.

that multiple vehicles attempt to contend, causing a collision at the RSU. After this contention period, the contention free period starts and all registered vehicles (including newly registered vehicles) switch their CCH channel to an SCH channel specified in the TAF.

Let O_c be the number of vehicles that send packets, and then the maximum CP length can be calculated as follows:

$$T_{CP}^{STMAC} = DIFS + TAF + (DIFS + REQ + SIFS + ACK) \cdot \sum_{i=O_c}^{1} \frac{1}{i \cdot p \cdot (1-p)^{i-1}} + SIFS + T_{CS} + T_{GI}, \quad (6)$$

where $DIFS$, TAF, REQ, $SIFS$, ACK, T_{CS}, and T_{GI} are the time for the DCF interframe space, the timing advertisement frame, the registration request frame, the short interframe space, the acknowledgement frame, the channel switch, and the guard interval, respectively, and $\sum_{i=O_c}^{1} \frac{1}{i \cdot p \cdot (1-p)^{i-1}}$ is the expected number of vehicle registrations derived in Section IV-B.

Note that during the CP phase, both registered and unregistered vehicles can transmit an emergency message to an RSU for emergency data dissemination (*e.g.*, accident notification).

B. CFP Phase for Driving Information Exchange

In a CFP phase, registered vehicles attempt exchange their driving safety information with their neighboring vehicles based on the contention-free schedule in service channels (SCHs). As shown in Fig. 8(b), a TAF containing the channel access schedule of registered vehicles is broadcasted by an RSU. Each vehicle based on the schedule in the TAF transmits its basic safety message (BSM) (*e.g.*, mobility information and vehicle internal states) to its intended receivers for the time slot. As shown in the dashed line box of Fig. 8(b), the transmissions of BSM packets are multiplexed in the time slots according to the spatio-temporal coordination described in Section IV-A. Let O_r^{STMAC} be the number of time slots allocated by the spatio-temporal coordination in a CFP; then, O_c vehicles may use O_r^{STMAC} time slots to exchange safety messages. Thus, the maximum length of a CFP in STMAC can be expressed as:

$$T_{CFP}^{STMAC} = PIFS + TAF + \sum_{i=1}^{O_r^{STMAC}} (SIFS + BSM_i) + SIFS + T_{CS} + T_{GI}, \quad (7)$$

where $PIFS$ and BSM_i are the time for the PCF interframe space and the basic safety message for vehicle i, respectively.

Using the NVs from the TAF, each vehicle constructs the coverage regions for its intended transmissions by the directional antenna and the transmission power control. Note that during the CFP phase, if the RSU has an emergency message, it can announce a TAF having emergency information.

Thus, by the CP and CFP phases, STMAC can allow for not only the fast exchange of driving safety information among vehicles, but also the fast dissemination of emergency data of the vehicles under the RSU.

C. Vehicle Mobility Information Update

In the STMAC protocol, the RSU periodically broadcasts a special TAF in a CP phase to collect the most current mobility information of all registered vehicles. This enables vehicles to correctly select the transmission direction and power control parameters by the latest position of a receiver vehicle. This TAF is also used to deregister vehicles that have left the communication range of the RSU, and which do not respond to this TAF. Each registered vehicle sends its updated mobility by transmitting a BSM, which includes its mobility information, to the RSU. The superframe for the vehicle mobility information update is repeated every U times, such as $U = 10$, considering the mobility prediction accuracy. With this update, the RSU estimates the vehicle's mobility in the near future (*e.g.*, after 100 milliseconds) for time slot scheduling.

D. Performance Analysis

We have so far explained the design of STMAC protocol. Now we analyze the performance of STMAC and WPCF. Since WPCF is the MAC protocol most similar to STMAC, we particularly study the performance of WPCF. Table I shows the performance analysis of STMAC and WPCF. The maximum CP and CFP lengths of STMAC were discussed in Sections V-A and V-B. Notice that the number of time slots (*i.e.*, O_r^{STMAC}) allocated in a CFP of STMAC is a result of the spatio-temporal coordination. The acknowledgement process between any two LoC vehicles, of which the time is $SIFS + ACK$, is removed to improve the efficiency of the safety information exchange. We assume that every vehicle has safety messages that must be sent. The superframe duration of STMAC can be described as

$$T_{SF}^{STMAC} = T_{CP}^{STMAC} + T_{CFP}^{STMAC}. \quad (8)$$

TABLE I
PERFORMANCE ANALYSIS OF STMAC AND WPCF

Scheme	Maximum CP Length (T_{CP})	Maximum CFP Length (T_{CFP})
STMAC	$DIFS + TAF + (DIFS + REQ + SIFS + ACK) \cdot \sum_{i=O_c}^{1} \frac{1}{i \cdot p \cdot (1-p)^{i-1}} + SIFS + T_{CS} + T_{GI}$	$PIFS + TAF + \sum_{i=1}^{O_r^{STMAC}} (SIFS + BSM_i) + SIFS + T_{CS} + T_{GI}$
WPCF [11]	$DIFS + TAF + (DIFS + REQ + SIFS + ACK) \cdot \sum_{i=O_c}^{1} \frac{1}{i \cdot p \cdot (1-p)^{i-1}} + SIFS + END$	$SIFS + TAF + \sum_{i=1}^{O_r} (WPIFS[1] + BSM_i + SIFS + ACK) + END$

The maximum CP length T_{CP}^{WPCF} of WPCF is similar to that of STMAC, but WPCF has no registration mechanism for continuous communications, which means that whenever a vehicle has a packet to send, it needs to reserve a time slot in a CP. Also, the vehicles with the WPCF scheme, which reserved the time slots in the CP, do not utilize the spatial feature to reduce the number of time slots. Thus, the maximum CFP length of WPCF is determined by the number of vehicles with reserved time slots in the CP. Note that the number of vehicles within the coverage of one RSU at an intersection is a reasonable number, so the CFP period will increase reasonably as the number of vehicles increases. Assume that there are O_r vehicles having packets to send; the maximum CFP length for these O_r vehicles is:

$$T_{CFP}^{WPCF} = SIFS + TAF + \sum_{i=1}^{O_r} \times (WPIFS[1] + BSM_i + SIFS + ACK) + END, \tag{9}$$

where $WPIFS$ is the WAVE PCF interframe space defined in WPCF [11]; $WPIFS[k] = SIFS + (k \times T_{slot})$; k is the sequence number for the transmission order of a vehicle in the current CFP schedule, and k is always 1 because every registered vehicle transmits its data frame to the RSU according to its transmission order in the schedule [11]; BSM_i is the transmission time of the basic safety message for a vehicle i; and END is the CFP end frame sent by an RSU, which can be equal to the $T_{CS} + T_{GI}$ of STMAC. Thus, the superframe duration T_{SF}^{WPCF} of WPCF is

$$T_{SF}^{WPCF} = T_{CP}^{WPCF} + T_{CFP}^{WPCF}. \tag{10}$$

To measure the interval between two consecutive safety messages which are transmitted by a vehicle and are received by its neighboring vehicles, we define E2E delay to describe it. Based on the superframe duration of STMAC and WPCF, the E2E delay of STMAC (denoted as T_{E2E}^{STMAC}) and that of WPCF (denoted as T_{E2E}^{WPCF}) can be estimated by the uniformly distributed channel access in both CP and CFP phases:

$$T_{E2E}^{STMAC} = \frac{T_{CFP}^{STMAC}}{2} + T_{CP}^{STMAC} + \frac{T_{CP}^{STMAC}}{2} = \frac{T_{SF}^{STMAC}}{2} + T_{CP}^{STMAC}. \tag{11}$$

$$T_{E2E}^{WPCF} = \frac{T_{CFP}^{WPCF}}{2} + T_{CP}^{WPCF} + \frac{T_{CP}^{WPCF}}{2} = \frac{T_{SF}^{WPCF}}{2} + T_{CP}^{WPCF}. \tag{12}$$

TABLE II
PARAMETERS FOR PERFORMANCE ANALYSIS

Parameter	Value
T_{slot}	13 μs
SIFS	32 μs
PIFS	45 μs (SIFS+T_{slot})
DIFS	58 μs (SIFS+$T_{slot} \times 2$)
$T_{CS} + T_{GI}$ (END)	4 ms
Data rate	6 Mbps
Size of TAF packet	800 bits + Payload
Size of BSM packet	1024 bits + 88 bits
Size of REQ packet	288 bits
Size of ACK packet	128 bits

We verified the analytical models of STMAC and WPCF by comparing the analytical results with the simulation results in Section VI-B based on the parameters in Table II. Note that the contents of a BSM can be modified to adapt to different scenarios, which may vary the size of a BSM.

Since it is a CSMA/CA-based MAC scheme, LMA does not have the concept of superframe. Thus, we cannot determine the superframe duration as we can for STMAC and WPCF. Note that many analysis models have been proposed (*e.g.*, Markov chain model [34]–[37]) to describe the performance of CSMA/CA schemes.

So far, we have explained the design of the STMAC protocol. In the next section, we will evaluate our STMAC with baselines in realistic settings.

VI. PERFORMANCE EVALUATION

In this section, we evaluate the performance of STMAC in terms of average superframe duration, E2E delay, and packet loss ratio as performance metrics. We set the data rate as 6 Mbps, and utilize the Nakagami-3 [27] radio model for both transmitter and receiver to support the irregularity of transmission coverage, interference, and path loss in vehicular environments. We assume that a transmission coverage can be optimized in STMAC from a design perspective for an optimized communication coverage. Also, multiple transmissions can be emitted toward multiple receivers by a transmitter's directional antenna.

The evaluation settings are as follows:

- **Performance Metrics:** We use (i) *Average superframe duration*, (ii) *E2E delay*, and (iii) *Packet loss ratio* as metrics for the performance.
- **Baseline:** LMA [10], WPCF [11], DMMAC [14], and EDCA [4] were used as baselines.

TABLE III
SIMULATION CONFIGURATION

Parameter	Description
Road network	The number of intersections is 11. The area of the road map is 500 m × 600 m (*i.e.*, 0.31 miles × 0.37 miles).
Number of vehicles (N)	The number of vehicles moving in the road network ranges from 50 to 300. The default is 150.
Communication range (R)	$R = 25 \sim 150$ meters (*i.e.*, $82.02 \sim 492.13$ feet). The default is 75 meters.
GPS location error (ϵ)	$\epsilon = 0 \sim 18$ meters (*i.e.*, $0 \sim 59$ feet). The default is 3 meters.
Maximum vehicle speed (v_{max})	Maximum vehicle speed (*i.e.*, speed limit) for road segments. The default is $22.22 m/s$ (*i.e.*, 49.7 MPH).
Radio delay (d_r)	The time taken to switch from Rx to Tx mode for OFDM PHY defined in IEEE 802.11-2012 [4]. The default is $1\mu s$.
Transmission power (P)	The value is variable, decided by equation (1) and Algorithm 1.
Data traffic rate	The frequency of safety information transmission. The default is 100 packets per second.

- **Parameters:** For the performance, we investigate the impacts of the following parameters: (i) *Vehicle number* (*i.e.*, Vehicle traffic density) N, (ii) *GPS position error* (*i.e.*, Vehicle location error) ϵ, (iii) *Radio antenna*, and (iv) *Contention period duration*.

We use a road network with 11 intersections associated with 11 RSUs from a rectangular area of Los Angeles, CA, USA using Open Street Map [38] as shown in Fig. 9. The total length of the road segments of the road network is about 4.92 km (*i.e.*, 3.06 miles). We built STMAC, WPCF, LMA, DMMAC, and EDCA using OMNeT++ [39] and Veins [40] as well as applying the settings specified in Table III. Veins is an open source software to simulate vehicle communication and networks, including signal fading models. Directional antenna coverage is formed by a directional antenna array [23] on top of a realistic wireless radio model in Veins, such as Nakagami fading model [27]. To use realistic vehicle mobility in the road network, we fed the vehicle mobility information to OMNeT++ using a vehicle mobility simulator called SUMO [41] via the TraCI protocol [41]. SUMO was extended such that vehicles move around, rather than escape from a target road network.

Because our objective is to show the performance of local communications among an RSU and vehicles in the same road segment, rather than the E2E delivery delay between two remote vehicles in a large-scale road network, the simulation topology shown in Fig. 9 is sufficient for evaluating our proposed protocol. The packets for safety messages continue to be generated during the travel of vehicles. We averaged 10 samples with confidence interval (*i.e.*, error bar) in the performance results.

A. Comparison of Data Delivery Behaviors

We compared the data delivery behaviors of STMAC, WPCF, LMA, DMMAC, and EDCA with the cumulative distribution function (CDF) of the superframe duration, E2E delay, and packet loss ratio. Fig. 10 shows that the CDF of STMAC reaches 100% much faster than those of WPCF, LMA, DMMAC, and EDCA. For example, STMAC has the average superframe duration of 0.021 s for 80% CDF, while for the same CDF value, WPCF has that of 0.052 s. Also, STMAC has the E2E delay of 0.017 s for 80% CDF while WPCF has that of 0.055 s and LMA has that of 1.2 s. In addition, The packet loss ratio of STMAC is 0.3% for 80% CDF. While that for WPCF is 25% and that for LMA is 1.8%. We observed that STMAC has better channel utilization, shorter E2E delay, and less packet loss ratio than WPCF, LMA, DMMAC, and EDCA. We show the forwarding performance of these three schemes quantitatively in the following subsections.

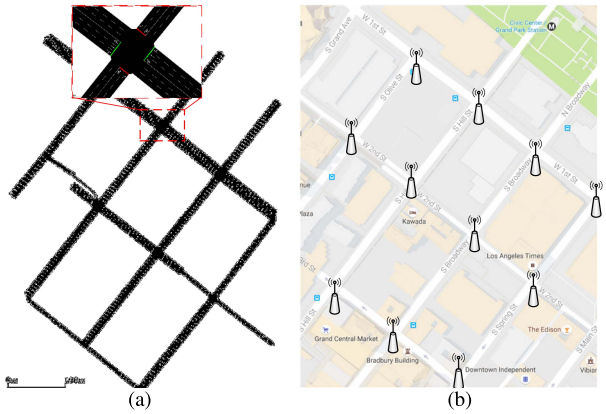

Fig. 9. Road network for simulation. (a) Extracted map in SUMO. (b) Real map with RSU placement.

B. Impact of Number of Vehicles

To examine the impact of the vehicle density, we varied the number of vehicles from 50 to 300 in the simulations. Since LMA, DMMAC, and EDCA do not have a superframe period, we only verified the analytical results of superframe duration and E2E delay of STMAC and WPCF.

Fig. 11(a) shows both the analytical and simulation results of the average superframe duration for the different vehicle densities. We obtained the analytical results from the analysis in Section V-D by uniformly assigning vehicles to each RSU. Note that the setting of uniformly distributed vehicles is used to get the performance results of the theoretical analysis in Section V-D. In the simulation, the vehicles are not uniformly distributed. The vehicle traffic is from SUMO which models a realistic vehicle mobility. Vehicles select their random destination and move to their destination in a shortest path. The results in Fig. 11(a) show that the simulation data match well with the analytical results. The average superframe duration of STMAC is shorter than that of WPCF. Especially, in a highly congested road situation, STMAC outperforms WPCF by 66.7%. It was observed that as the vehicle density increases, a small gap appears between the simulation and the analytical data of WPCF. This is due to the non-uniform vehicle distribution in the simulation. A small gap between the simulation result and analytical result of STMAC is also observed, but due to the scale of the figure, such a gap is not

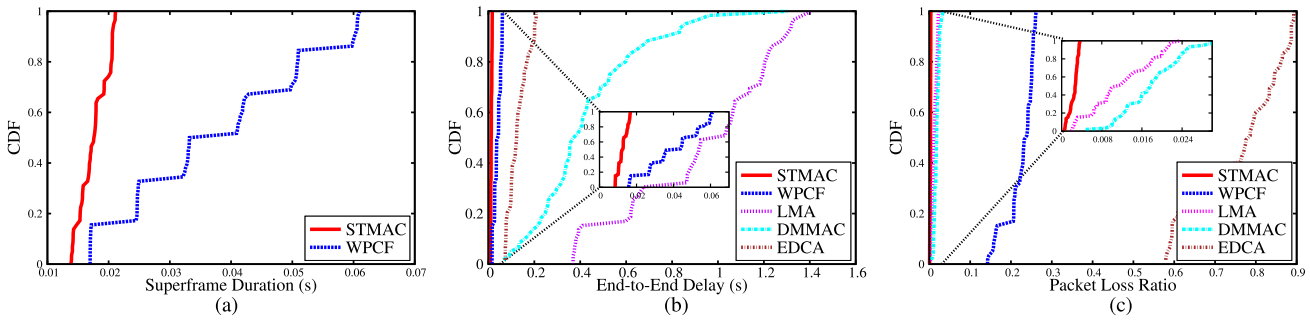

Fig. 10. CDF of superframe duration, E2E delay and packet loss ratio for STMAC, WPCF, and LMA. (a) CDF of superframe duration. (b) CDF of E2E delay. (c) CDF of packet loss ratio.

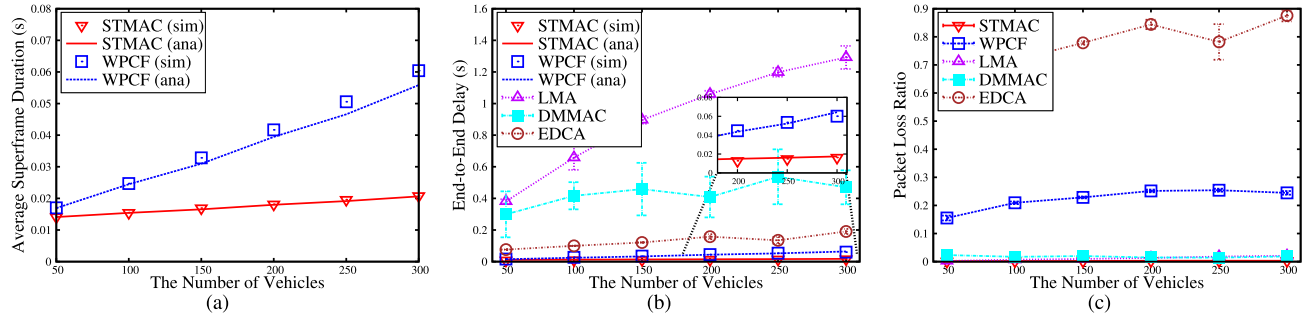

Fig. 11. Impact of the number of vehicles. (a) Average superframe duration for STMAC and WPCF. (b) Packet E2E delay for STMAC, WPCF, and LMA. (c) Packet loss ratio for STMAC, WPCF, and LMA.

significant. Notice that in Fig. 11(a), the curve of STMAC is linearly increasing rather than constant according to the increase of vehicles. Also, note that the average superframe duration determines the time duration of a vehicles safety information transmission toward its adjacent vehicles in the LoC graph. Thus, the shorter average superframe duration indicates the more often exchange of safety information among vehicles.

As described in Section V-D, the average superframe duration determines the packet E2E delay. Fig. 11(b) shows the analytical and simulation results of the average E2E delay of packet delivery. Overall, the simulation results show a good agreement with the analytical results, as shown in the small window of Fig. 11(b). As the number of vehicles increases, all of STMAC, WPCF, LMA, DMMAC, and EDCA have a longer average E2E delay. In any road traffic condition (*i.e.*, $N = 50$ through $N = 300$), STMAC has a shorter packet E2E delay than WPCF, LMA, DMMAC, and EDCA due to both the optimized CP duration and concurrent transmissions by spatio-temporal coordination. Especially, for highly congested road traffic of $N = 300$, the packet E2E delay of STMAC is one third of WPCF's delay. Notice that the E2E delay of LMA is identical to the result reported in LMA [10]. LMA has much higher E2E delays than those of STMAC and WPCF in all vehicle densities. This is due to the mechanism of CSMA/CA [4] that can let multiple control frames experience collision before the transmission of a data frame.

Fig. 11(c) shows the packet loss ratio according to the increasing number of vehicles. In all vehicle densities from 50 to 300, STMAC has a much lower packet loss ratio than both WPCF, LMA, DMMAC, and EDCA since in STMAC, vehicles can communicate with their LoC vehicles by an optimized communication range. Even for highly congested road traffic of $N = 300$, STMAC gains a packet loss ratio less than 1%, but the packet loss ratios of WPCF and LMA are 24% and 2.5%, respectively. Through the observation of the simulations, the high packet loss ratio of WPCF is caused by signal attenuation and the packet collisions in handover areas. The packet loss of LMA, which lacks spatial coordination, is produced mainly by the packet collisions between the data frames and the control frames. The spatial coordination and the transmission power control induce a very low packet loss ratio for STMAC.

From the performance comparison of the superframe duration, the E2E delay, and the packet loss ratio, STMAC outperforms the other state-of-the-art schemes considerably, indicating that it can support reliable and fast safety message exchange. These improvements are because STMAC allows vehicles to transmit their safety information frames to their neighboring vehicles in the LoC graph through spatio-temporal coordination in an RSU in a direct V2V communication. This coordination can reduce the frame collision and the direct V2V communication reduces the data delivery delay between vehicles. On the other hand, LMA lets vehicles access the wireless channel randomly, so this increases the frame collision probability as the number of vehicles increases. Also, since WPCF does not consider CP duration optimization unlike STMAC, the channel utilization of WPCF is worse than that of STMAC.

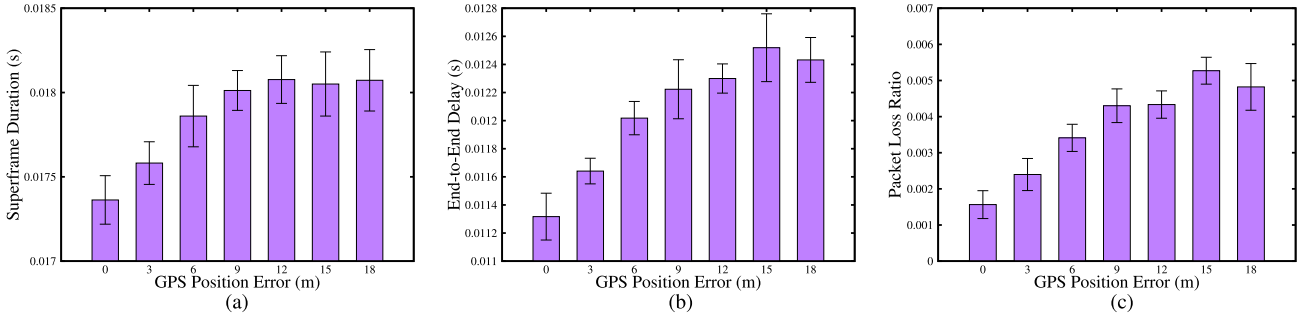

Fig. 12. Impact of GPS position error. (a) Average superframe duration. (b) Packet E2E delay. (c) Packet loss ratio.

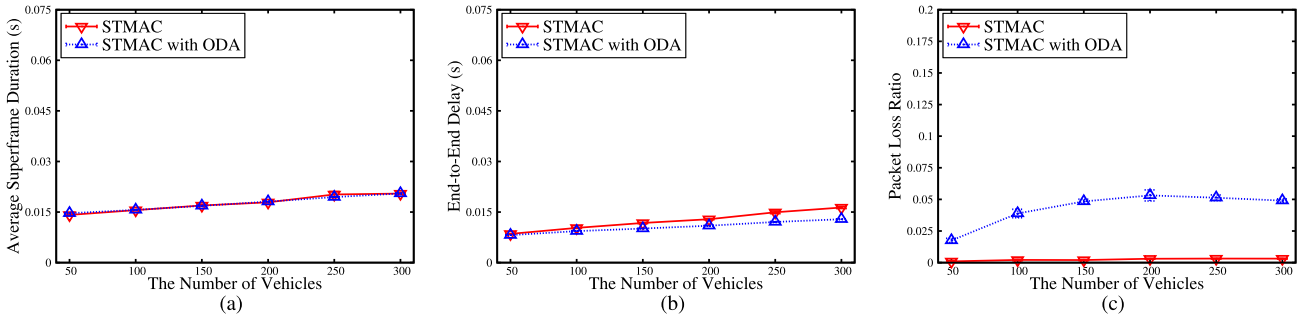

Fig. 13. Impact of radio antenna. (a) Average superframe duration with omni-directional antenna. (b) Packet E2E delay with omni-directional antenna. (c) Packet loss ratio with omni-directional antenna.

C. Impact of GPS Position Error

In an urban area, tall buildings usually seriously affect the precision of GPS localization, which can also influence the performance of STMAC since STMAC utilizes the coordinates of vehicles to schedule time slots. Therefore, we evaluated the performance of STMAC by varying the GPS position error at a medium vehicle density (*i.e.*, 150 vehicles). Fig. 12 shows the average superframe duration, E2E delay, and packet loss ratio according to GPS position error. The average superframe duration of STMAC increases as the GPS error increases, as shown in Fig. 12(a), but as the error reaches above 9 meters, the average superframe duration remains stable. The worst case occurred at the GPS position error with 12 meters, where the average superframe duration is about 18.1 ms, which is still within a safe driving range (*e.g.*, 100 ms [42]). On the other hand, as the GPS error increases, the E2E delay also increases as shown in Fig. 12(b), and the worst case is about 12.5 ms on average. For packet loss ratio, in the zero GPS position error, STMAC performs with less than 0.18% packet loss ratio, and gains increased packet loss ratio as the GPS error range increases. From the result shown in this figure, it is expected that STMAC can work well for safety message exchange [42] even in urban road networks with a high GPS error due to buildings. The good tolerance of GPS error in STMAC benefits from the design of STMAC protocol. Algorithm 1 considers the GPS error when using the vehicles position information to schedule the transmissions. Based on the algorithm, vehicles transmit data following the enlarged transmission range to compensate the impact of GPS error.

D. Impact of Radio Antenna

To evaluate the impact of radio antenna, we conducted simulations by switching the radio antenna. Fig. 13 shows the impact of radio antenna, such as directional antenna and omni-directional antenna (ODA). As shown in Fig. 13(a), STMAC using directional antenna has almost the same superframe duration as that of STMAC using ODA. For packet E2E delay, as shown in Fig. 13(b), STMAC using directional antenna has slightly longer E2E delay than STMAC using ODA. This is because vehicles using ODA in STMAC exchange safety messages with adjacent vehicles when updating their mobility information to RSUs; this update reduces the E2E delay of safety messages.

For data packet loss ratio, as shown in Fig. 13(c), the data packet loss ratio of STMAC with directional antenna is less than that of STMAC with ODA. The data packet loss of STMAC with ODA is due to two factors: signal attenuation and the packet loss in handover areas. The packet loss in handover areas results from the channel switch of vehicles in the handover areas. Assume that vehicle A (V_A) that is moving into a handover area becomes registered in a new RSU (RSU_n) and its service channel is switched according to RSU_n. The predecessor RSU (RSU_p) of V_A can still generate transmission schedules including V_A until the next update period. The other vehicles in RSU_p receiving the schedules can transmit their data packets to V_A in the handover area, although V_A has switched from the service channel of RSU_p to the service channel of RSU_n. The vehicles with ODA in RSU_p can increase the data packet loss in the handover areas, since V_A in the handover area can receive more data packets from the

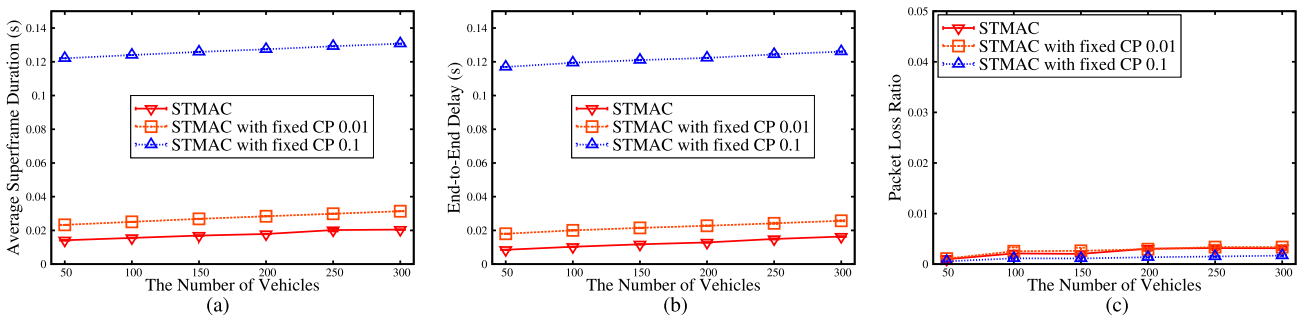

Fig. 14. Impact of contention period duration. (a) Average superframe duration for CP duration. (b) Packet E2E delay for CP duration. (c) Packet loss ratio for CP duration.

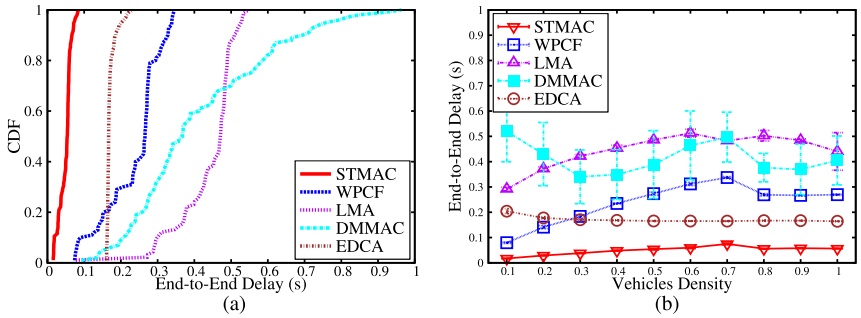

Fig. 15. Performance in highly congested scenario. (a) CDF of E2E delay at one intersection. (b) Packet E2E delay at one intersection.

vehicles with ODA than from the vehicles with directional antenna. However, this data packet loss does not affect the average packet E2E delay, because the vehicles in handover areas can receive data packet correctly from the other vehicles in the coverage of RSU_n, as shown in Fig. 13(b).

The results in Fig. 13 indicate that STMAC with directional antenna can significantly reduce packet loss while maintaining a good packet E2E delay in comparison with STMAC with omni-directional antenna.

E. Impact of Contention Period Duration

We also fixed the length of the CP to show the impact of the contention period duration. Particularly, we select 100 *ms* and 10 *ms* for the fixed-length CP to evaluate the performance of STMAC with the CP adaptation. Fig. 14 shows the impact of CP duration in STMAC. For average superframe duration, as shown in Fig. 14(a), the E2E delay of STMAC with CP adaptation has shorter average superframe duration than STMAC with constant CP duration (*i.e.*, 0.01*s* and 0.1 *s*, respectively). For packet E2E delay with CP adaptation, as shown in Fig. 14(b), the E2E delay of STMAC with CP adaptation is shorter than that of STMAC with both constant CP durations. For packet loss ratio with CP adaptation, as shown in Fig. 14(c), STMAC has small packet loss regardless of CP adaptation. This small packet loss ratio benefits from the directional antenna that reduces packet collisions.

F. Performance in Highly Congested Scenario

To measure the scalability of STMAC, we performed a simulation in a highly congested scenario at one intersection with four road segments. The intersection has three lanes on each road segment, and the length of each road segment is 300 meters. An RSU is placed at the intersection. Consider a vehicle with 5 meters length, and the minimum gap between two vehicles is 2.5 meters. To fully occupy the intersection, about 922 vehicles are required at the intersection. Fig. 15 shows the E2E delay performance among STMAC, WPCF, LMA, DMMAC, and EDCA. STMAC obtained the best performance on the E2E delay, which shows that the scalability of STMAC is good. In Fig. 15(a), the packet E2E delay of STMAC is always within 100 *ms* even in the full congested scenario, which can fulfill the minimum requirement for driving safety information exchange. Fig. 15(b) shows the trend of the packet E2E delay from a low density to a high density. With the increase of vehicle density, the packet E2E delays in STMAC, WPCF, and LMA also increase. The packet E2E delay of STMAC is much lower than those of WPCF and LMA, which is gained by the enhanced set-cover algorithm and the new hybrid MAC protocol utilizing the spatio-temporal coordination. Also, notice that the E2E delays in STMAC and WPCF reach the highest point at the vehicle density with 0.7. After the peak, the E2E delay maintains as almost constant. Based on the observation, the peak indicates the saturation scenario within the coverage of the RSU. When vehicle density is larger than 0.7, the intersection experiences traffic jam that hinders vehicles to move into the coverage of the RSU, which reduces the E2E delay.

Therefore, the results from the performance evaluation show that STMAC is a promising MAC protocol for driving safety to support the reliable and rapid exchange of safety messages among nearby vehicles.

VII. Conclusion

In this paper, we propose a Spatio-Temporal Coordination based Media Access Control (STMAC) protocol in an urban area for an optimized wireless channel access. We characterize the spatio-temporal feature using a line-of-collision (LoC) graph. With this spatio-temporal coordination, STMAC organizes vehicles that transmit safety messages to their neighboring vehicles reliably and rapidly. Vehicles access wireless channels in STMAC, combining the merits of the PCF and DCF modes. In the PCF mode, the vehicles register their mobility information in RSU for time slot reservation, and they then receive their channel access time slots from a beacon frame transmitted by an RSU. In the DCF mode, the vehicles concurrently transmit their safety messages to their neighboring vehicles through the spatio-temporal coordination. We theoretically analyzed the performance of STMAC, and conducted extensive simulations to verify the analysis. The results show that STMAC outperforms the legacy MAC protocols using either PCF or DCF mode even in a highly congested road traffic condition. Thus, through STMAC, a new perspective for designing a MAC protocol for driving safety in vehicular environments is demonstrated.

For future work, we will extend our STMAC to support data services (*e.g.*, multimedia streaming and interactive video call) for high data throughput rather than for short packet delivery time. Also, we will study a traffic-light-free communication protocol for autonomous vehicles passing intersection without the coordination of a traffic light. For a highway scenario, we will study an efficient communication protocol for driving safety.

Appendix A
Contention Period Adaptation

For a particular number of vehicles N, we can find an optimal p that can give the best successful probability g_N for each vehicle to send a registration request, so through

$$\frac{dg_N}{dp} = N \cdot (1-p)^{N-1} - N \cdot (N-1) \cdot p \cdot (1-p)^{N-2} = 0, \tag{13}$$

we can obtain an optimal p:

$$p = \frac{1}{N}. \tag{14}$$

Accordingly, the optimal g_N is:

$$g_N = (1 - \frac{1}{N})^{N-1}. \tag{15}$$

The average number of slots to register one vehicle among N vehicles based on Equation (4) is:

$$M_N = \frac{1}{g_N} = \frac{1}{N \cdot p \cdot (1-p)^{N-1}}. \tag{16}$$

After a vehicle is registered with M_N, M_{N-1} for only $N-1$ vehicles is computed in the same way:

$$M_{N-1} = \frac{1}{g_{N-1}} = \frac{1}{(N-1) \cdot p \cdot (1-p)^{N-2}}. \tag{17}$$

Therefore, the total number of slot to register N vehicles is:

$$M = \sum_{i=N}^{1} \frac{1}{g_i} = \sum_{i=N}^{1} \frac{1}{i \cdot p \cdot (1-p)^{i-1}}. \tag{18}$$

Appendix B
Maximum Compatible Set Algorithm

To construct a set-cover, the STMAC-Set-Cover algorithm in Algorithm 1 searches for a maximum compatible cover-set, using $Search_Max_Compatible_Cover_Set(G, E')$ with the LoC graph G and the edge set E' in Algorithm 2. The remaining edges of this edge set E' are used for further compatible cover-sets for concurrent communications in G.

Algorithm 2 Search-Max-Compatible-Cover-Set Algorithm

```
1: function SEARCH_MAX_COMPATIBLE_COVER_SET (G, E')  ▷ G is the LoC graph and E' is the set of the remaining edges not belonging to any cover-set
2:     V' ← ∅                ▷ V'(⊆ V) is for a set of vertices with directed edges in E' and initialized with ∅
3:     M_max ← ∅             ▷ M_max is for a maximum compatible cover-set and initialized with zero
4:     for all edges e_{i,j} ∈ E' do
5:         V' ← V' ∪ {v_i, v_j}
6:     end for
7:     for each vertex s ∈ V' do
8:         M ← Make_Maximal_Compatible_Set(G, V', E', s)
9:         if |M_max| < |M| then
10:            M_max ← M
11:        end if
12:    end for
13:    return M_max
14: end function
```

Algorithm 2 searches for a maximum compatible cover-set among maximal compatible cover-sets constructed by $Make_Maximal_Compatible_Set$ (G, V', E', s) in Algorithm 3. Algorithm 2 takes as input E' that is a set of edges not belonging to any compatible cover-set and it returns the maximum compatible cover-set, M_{max}. V' is for a set of vertices with directed edges in E'. Lines 2-3 initialize the V' and M_{max} to $\emptyset$. In lines 4-6, V' is a set of vertices such that v_i and v_j are linked with any directed edges $e_{i,j}$ in E'. For each vertex s in V' as a start node (*i.e.*, root vertex) for breadth-first search (BFS) [21], we find a candidate maximal compatible set, M. In lines 7-12, if the number of elements in M is bigger than that of M_{max}, M is set to M_{max}. After running the for-loop in lines 7-12, consequently, M_{max} is returned as a maximum compatible cover set for the given edge set E'.

Algorithm 3 computes a maximal compatible cover set with s as a starting vertex for BFS along with interference range. The input parameters in Algorithm 3 are G as the LoC graph, V' as the set of vertices for the remaining edges in E', E' as the remaining edge set, and s as a start node for BFS in the subgraph corresponding to $G(V', E')$.

Algorithm 3 Make-Maximal-Compatible-Set Algorithm

```
1: function MAKE_MAXIMAL_COMPATIBLE_SET (G, V', E', s)  ▷ G is the LoC graph, V' is the set of vertices with directed edges in E', E' is the remaining edge set, and s is a start node for breadth-first search
2:   G' ← Graph(V', E')
3:   G'' ← Undirected_Graph(G')
4:   E_max ← ∅
5:   T ← ∅
6:   I ← ∅
7:   for each vertex u ∈ V' − {s} do
8:     u.color ← WHITE
9:     u.degree ← 0
10:    u.receivers ← ∅
11:  end for
12:  s.color ← GRAY
13:  s.degree ← 0
14:  Q ← ∅
15:  Enqueue(Q, s)
16:  while Q ≠ ∅ do
17:    u ← Dequeue(Q)
18:    count ← 0
19:    I ← Interference_Set(G, T)
20:    for each vertex v ∈ N_G''(u) do
21:      if (v.color = WHITE) or (v.color = GRAY and v.degree = 0) then
22:        if v ∈ N_G'(u) and u.degree = 0 and v ∉ I then
23:          E_max ← E_max ∪ {e_uv}
24:          v.degree ← 1
25:          count ← count + 1
26:          u.receivers ← u.receivers ∪ {v}
27:        end if
28:        v.color ← GRAY
29:        Enqueue(Q, v)
30:      end if
31:    end for
32:    if count > 0 then
33:      u.degree ← count
34:      u.color ← BLACK
35:      T ← T ∪ {u}
36:    end if
37:  end while
38:  return E_max
39: end function
```

Lines 5-6 make a transmission set and an interference set for a tripartite graph about the relationship between transmitters and interfered vehicles via each transmitter's receivers. In line 5, a transmission set T will contain transmitters in the compatible cover-set in the LoC subgraph G' for the current time slot. In line 6, an interference set I will contain vehicles which get the interference from a transmitter $t \in T$ in the LoC graph G. In lines 7-11, the color and degree of each vertex $u \in V' - \{s\}$ are set to $WHITE$ as an unvisited vertex and 0, respectively. Also, the set of u's receivers (*i.e.*, $u.receivers$) is set to $\emptyset$. In lines 12-13, the color and degree of the start node s are set to $GRAY$ and 0, respectively. In lines 14-15, a first-in-first-out (FIFO) queue Q is constructed, and the start node s is enqueued for BFS. In lines 16-37, edges $e_{uv} \in E'$ are added to the maximal compatible cover-set E_{max}. In lines 17-18, u is the front vertex dequeued from Q and $count$ for u's outgoing degree is initialized with 0. Remarkably, in line 19, an interference set I is computed by $Interference_Set(G, T)$ along with the current transmission set T in the compatible cover-set for a time slot on the LoC graph G. For each transmitter $t \in T$, $Interference_Set(G, T)$ searches for white, interfered vertices $i \in I$ that are adjacent to t's receiver in the LoC G. In lines 20-31, for each vertex v that is an adjacent vertex to u in the undirected LoC subgraph G'', it is determined to add the edge e_{uv} to E_{max} by checking whether or not the receiver v is under the interference of any vertex $i \in I$. In lines 21-30, if v is a white vertex (*i.e.*, unvisited vertex) or a gray vertex with its degree 0 (*i.e.*, visited vertex, but neither transmitter nor receiver), and also if v is an adjacent vertex to u in the directed LoC subgraph G', u has not yet been selected as a transmitter, and v is not under the interference of any other vertex $i \in I$, then the edge e_{uv} is added to E_{max}, v's incoming degree is set to 1, u's outgoing degree increases by 1 with $count$, v is added to the u's receiver set $u.receivers$, and v is enqueued into Q for the further expansion of the BFS tree. Otherwise, if v is only a white vertex and the condition in line 22 is false, then v is enqueued into Q for the further expansion of the BFS tree. In lines 32-36, if the $count$ is positive, then u's outgoing degree is set to $count$, and u is added to the transmission set T as a black vertex. Finally, after finishing the while-loop in lines 16-37, a maximal compatible cover-set E_{max} is returned.

REFERENCES

[1] J. Harding *et al.*, "Vehicle-to-vehicle communications: readiness of V2V technology for application," Nat. Highway Traffic Safety Admin., Washington, DC, USA, Tech. Rep. DOT HS 812 014, 2014.

[2] Y. L. Morgan, "Notes on DSRC & WAVE standards suite: Its architecture, design, and characteristics," *IEEE Commun. Surveys Tuts.*, vol. 12, no. 4, pp. 504–518, 4th Quart., 2010.

[3] ASTM International, "Standard specification for telecommunications and information exchange between roadside and vehicle systems −5 GHz band dedicated short range communications (DSRC) medium access control (MAC) and physical layer (PHY) specifications," ASTM, West Conshohocken, PA, USA, Tech. Rep. ASTM E2213-03(2010), 2010, pp. 1–25.

[4] *IEEE Standard for Information Technology–Telecommunications and Information Exchange Between Systems Local and Metropolitan Area Networks–Specific Requirements Part 11: Wireless LAN Medium Access Control (MAC) and Physical Layer (PHY) Specifications*, IEEE Standard 802.11-2012 and IEEE Standard 802.11-2007, Mar. 2012, pp. 1295–1303.

[5] *IEEE Guide for Wireless Access in Vehicular Environments (WAVE)—Architecture*, IEEE Standard 1609.0-2013, Mar. 2014, pp. 1–78.

[6] S. Eichler, "Performance evaluation of the IEEE 802.11p WAVE communication standard," in *Proc. IEEE 66th Veh. Technol. Conf.*, Sep. 2007, pp. 2199–2203.

[7] Z. Wang and M. Hassan, "How much of DSRC is available for non-safety use?" in *Proc. 5th ACM Int. Workshop Veh. Inter-NETworking (VANET)*, New York, NY, USA, 2008, pp. 23–29.

[8] S. Subramanian, M. Werner, S. Liu, J. Jose, R. Lupoaie, and X. Wu, "Congestion control for vehicular safety: Synchronous and asynchronous MAC algorithms," in *Proc. 9th ACM Int. Workshop Veh. Inter-NETworking, Syst., Appl. (VANET)*, New York, NY, USA, 2012, pp. 63–72.

[9] T. V. Nguyen, F. Baccelli, K. Zhu, S. Subramanian, and X. Wu, "A performance analysis of CSMA based broadcast protocol in VANETs," in *Proc. IEEE INFOCOM*, Apr. 2013, pp. 2805–2813.

[10] K.-T. Feng, "LMA: Location- and mobility-aware medium-access control protocols for vehicular ad hoc networks using directional antennas," *IEEE Trans. Veh. Technol.*, vol. 56, no. 6, pp. 3324–3336, Nov. 2007.

[11] J.-M. Chung, M. Kim, Y.-S. Park, M. Choi, S. Lee, and H. S. Oh, "Time coordinated V2I communications and handover for WAVE networks," *IEEE J. Sel. Areas Commun.*, vol. 29, no. 3, pp. 545–558, Mar. 2011.

[12] Y.-B. Ko, V. Shankarkumar, and N. H. Vaidya, "Medium access control protocols using directional antennas in ad hoc networks," in *Proc. IEEE INFOCOM*, vol. 1. Mar. 2000, pp. 13–21.

[13] Q. Wang, S. Leng, H. Fu, and Y. Zhang, "An IEEE 802.11p-based multichannel MAC scheme with channel coordination for vehicular ad hoc networks," *IEEE Trans. Intell. Transp. Syst.*, vol. 13, no. 2, pp. 449–458, Jun. 2012.

[14] K. A. Hafeez, L. Zhao, J. W. Mark, X. Shen, and Z. Niu, "Distributed multichannel and mobility-aware cluster-based MAC protocol for vehicular ad hoc networks," *IEEE Trans. Veh. Technol.*, vol. 62, no. 8, pp. 3886–3902, Oct. 2013.

[15] D. N. M. Dang, C. S. Hong, S. Lee, and E.-N. Huh, "An efficient and reliable MAC in VANETs," *IEEE Commun. Lett.*, vol. 18, no. 4, pp. 616–619, Apr. 2014.

[16] V. Nguyen, T. Z. Oo, P. Chuan, and C. S. Hong, "An efficient time slot acquisition on the hybrid TDMA/CSMA multichannel MAC in VANETs," *IEEE Commun. Lett.*, vol. 20, no. 5, pp. 970–973, May 2016.

[17] J. Lee and C. M. Kim, "A roadside unit placement scheme for vehicular telematics networks," in *Proc. LNCS*, vol. 6059. 2010, pp. 196–202.

[18] P. G. Lopez *et al.*, "Edge-centric computing: Vision and challenges," *SIGCOMM Comput. Commun. Rev.*, vol. 45, no. 5, pp. 37–42, Sep. 2015.

[19] Garmin Ltd. *Garmin Automotive*, accessed on 2017. [Online]. Available: https://www.garmin.com/en-US/

[20] Waze. *Waze Smartphone App for Navigator*, accessed on 2017. [Online]. Available: https://www.waze.com

[21] T. H. Cormen, C. E. Leiserson, R. L. Rivest, and C. Stein, *Introduction to Algorithms*, 3rd ed. Cambridge, MA, USA: MIT Press, 2009.

[22] K. Kim, J. Lee, and W. Lee, "A MAC protocol using road traffic estimation for infrastructure-to-vehicle communications on highways," *IEEE Trans. Intell. Transp. Syst.*, vol. 14, no. 3, pp. 1500–1509, Sep. 2013.

[23] M. S. Sharawi, F. Sultan, and D. N. Aloi, "An 8-element printed V-shaped circular antenna array for power-based vehicular localization," *IEEE Antennas Wireless Propag. Lett.*, vol. 11, pp. 1133–1136, 2012.

[24] D. Gesbert, M. Kountouris, R. W. Heath, Jr., C.-B. Chae, and T. Sälzer, "Shifting the MIMO paradigm," *IEEE Signal Process. Mag.*, vol. 24, no. 5, pp. 36–46, Sep. 2007.

[25] N. Razavi-Ghods, M. Abdalla, and S. Salous, "Characterisation of MIMO propagation channels using directional antenna arrays," in *Proc. 5th IEE Int. Conf. 3G Mobile Commun. Technol.*, Oct. 2004, pp. 163–167.

[26] V. Kawadia and P. R. Kumar, "Principles and protocols for power control in wireless ad hoc networks," *IEEE J. Sel. Areas Commun.*, vol. 23, no. 1, pp. 76–88, Jan. 2005.

[27] F. Schmidt-Eisenlohr, M. Torrent-Moreno, T. Mittag, and H. Hartenstein, "Simulation platform for inter-vehicle communications and analysis of periodic information exchange," in *Proc. 4th Annu. Conf. Wireless Demand Netw. Syst. Ser.*, Jan. 2007, pp. 50–58.

[28] New York State Department of Motor Vehicles. *Driver's Manual*, accessed on 2017. [Online]. Available: https://dmv.ny.gov/

[29] K. Xu, M. Gerla, and S. Bae, "How effective is the IEEE 802.11 RTS/CTS handshake in ad hoc networks," in *Proc. IEEE Global Telecommun. Conf. (GLOBECOM)*, vol. 1. Nov. 2002, pp. 72–76.

[30] L. G. Roberts, "ALOHA packet system with and without slots and capture," *ACM SIGCOMM Comput. Commun. Rev.*, vol. 5, no. 2, pp. 28–42, 1975.

[31] W. Crowther, R. Rettberg, D. Waldem, S. Ornstein, and F. Heart, "A system for broadcast communication: Reservation-ALOHA," in *Proc. 6th Hawaii Internat. Conf. Sist. Sci.*, Jan. 1973, pp. 596–603.

[32] R. K. Lam and P. R. Kumar, "Dynamic channel reservation to enhance channel access by exploiting structure of vehicular networks," in *Proc. IEEE 71st Veh. Technol. Conf. (VTC-Spring)*, May 2010, pp. 1–5.

[33] *IEEE Standard for Wireless Access in Vehicular Environments (WAVE)—Multi-Channel Operation, 1609 WG—Dedicated Short Range Communication Working Group*, IEEE Standard 1609.4-2016 and IEEE Standard 1609.4-2010, Mar. 2016, pp. 1–94.

[34] G. Bianchi, "Performance analysis of the IEEE 802.11 distributed coordination function," *IEEE J. Sel. Areas Commun.*, vol. 18, no. 3, pp. 535–547, Mar. 2000.

[35] J. Hui and M. Devetsikiotis, "A unified model for the performance analysis of IEEE 802.11e EDCA," *IEEE Trans. Commun.*, vol. 53, no. 9, pp. 1498–1510, Sep. 2005.

[36] Z.-N. Kong, D. H. K. Tsang, B. Bensaou, and D. Gao, "Performance analysis of IEEE 802.11e contention-based channel access," *IEEE J. Sel. Areas Commun.*, vol. 22, no. 10, pp. 2095–2106, Dec. 2004.

[37] Y. Yao, L. Rao, X. Liu, and X. Zhou, "Delay analysis and study of IEEE 802.11 p based DSRC safety communication in a highway environment," in *Proc. IEEE INFOCOM*, Apr. 2013, pp. 1591–1599.

[38] OpenStreetMap. *Open Street Map for Road Maps*, accessed on 2017. [Online]. Available: http://www.openstreetmap.org

[39] OMNeT++. *Network Simulation Framework*, accessed on 2017. [Online]. Available: http://www.omnetpp.org

[40] C. Sommer, R. German, and F. Dressler, "Bidirectionally coupled network and road traffic simulation for improved IVC analysis," *IEEE Trans. Mobile Comput.*, vol. 10, no. 1, pp. 3–15, Jan. 2011.

[41] D. Krajzewicz, J. Erdmann, M. Behrisch, and L. Bieker, "Recent development and applications of SUMO—Simulation of Urban MObility," *Int. J. Adv. Syst. Meas*, vol. 5, nos. 3–4, pp. 128–138, Dec. 2012.

[42] T. K. Mak, K. P. Laberteaux, and R. Sengupta, "A multi-channel VANET providing concurrent safety and commercial services," in *Proc. 2nd ACM Int. Workshop Veh. Ad Hoc Netw. (VANET)*, New York, NY, USA, 2005, pp. 1–9.

Jaehoon (Paul) Jeong (M'12) received the B.S. degree from the Department of Information Engineering, Sungkyunkwan University, in 1999, the M.S. degree from the School of Computer Science and Engineering, Seoul National University, South Korea, in 2001, and the Ph.D. degree from the Department of Computer Science and Engineering, University of Minnesota, in 2009. He is currently an Assistant Professor with the Department of Software, Sungkyunkwan University. His research interests include Internet of Things, vehicular networks, wireless sensor networks, and mobile ad hoc networks. He is a member of the ACM and the IEEE Computer Society.

Yiwen (Chris) Shen received the B.S. degree from the Department of Communication Engineering, North University of China, in 2009, and the M.S. degree from the Department of Mechatronics Engineering, North University of China, in 2013. He is currently pursuing the Ph.D. degree with the Department of Computer Science & Engineering, Sungkyunkwan University, South Korea. His research interests include intelligent transportation systems, vehicular ad hoc networks, and wireless communications. He received the China State Scholarship from the China Scholarship Council.

Sangsoo Jeong received the B.S. degree from the Department of Computer Software, Gachon University, Seongnam, South Korea, in 2013. He is currently pursuing the Ph.D. degree with the Department of Information and Communication Engineering, DGIST. His research areas include cyber-physical systems, smart city, vehicular ad hoc network (VANET), and Internet of Things (IoT).

Sejun Lee received the B.S. degree from the School of Information and Communication Engineering, Mokpo National Maritime University, South Korea, in 2014, and the M.S. degree from the Department of Computer Science and Engineering, Sungkyunkwan University, South Korea, under the supervision of J. Jeong. He is currently a Researcher with the Korea Electronics Technology Institute. His research areas include vehicular ad-hoc networks, cyber-physical systems, and internet of things.

Hwanseok (Harrison) Jeong (S'14) received the B.S. degree from the Department of Computer Engineering, Kyungpook National University, in 1999, and the M.S. degree from the School of Computer Science and Engineering, Seoul National University, in 2001. He is currently pursuing the Ph.D. degree with the Department of Computer Engineering, Sungkyunkwan University. He has been with SK Telecom as a Research and Development Strategist, and the Technical Engineer in Seoul, South Korea, since 2001. His research interests include vehicular ad-hoc networks, mobile ad hoc networks, and cyber-physical systems.

Tae (Tom) Oh (SM'09) received the B.S. degree in electrical engineering from Texas Tech University in 1991, and the M.S. and Ph.D. degrees in electrical engineering from Southern Methodist University in 1995 and 2001, respectively, while working for telecommunication and defense companies. He is currently an Associate Professor with the Department of Information Sciences and Technologies and the Department of Computing Security, Rochester Institute of Technology. His research includes mobile ad hoc networks, vehicle area networks, sensor networks, and mobile device security. He is a member of the ACM.

Taejoon Park (M'05) received the B.S. degree in electrical engineering from Hongik University, Seoul, South Korea, in 1992, the M.S. degree in electrical engineering from the Korea Advanced Institute of Science and Technology Daejeon, South Korea, in 1994, and the Ph.D. degree in electrical engineering and computer science from the University of Michigan, Ann Arbor, MI, USA, in 2005. He is currently a Professor with the Department of Robotics Engineering, Hanyang University, South Korea. His current research interests include in cyber-physical systems, Internet of Things, and their applications to robots and vehicles. He is a member of the ACM.

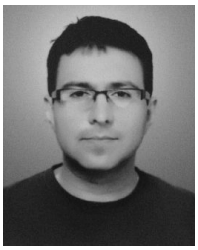

Muhammad Usman Ilyas received the B.E. degree (Hons.) in electrical engineering from the National University of Sciences and Technology (NUST), Islamabad, Pakistan, in 1999, the M.S. degree in computer engineering from the Lahore University of Management Sciences, Lahore, Pakistan, in 2004, and the M.S. and Ph.D. degrees in electrical engineering from Michigan State University in 2007 and 2009, respectively. He is currently appointed as an Assistant Professor of Electrical Engineering with the School of Electrical Engineering and Computer Science, NUST. He is also an Assistant Professor in the Department of Computer Science in the Faculty of Computing and Information Technology, University of Jeddah in Saudi Arabia.

Sang Hyuk Son (F'13) received the B.S. degree in electronics engineering from Seoul National University, the M.S. degree from KAIST, and the Ph.D. degree in computer science from the University of Maryland at College Park, College Park. He is currently the President of DGIST. He has been a Professor with the Computer Science Department, University of Virginia, and the WCU Chair Professor with Sogang University. His research interests include cyber physical systems, real-time and embedded systems, database and data services, and wireless sensor networks.

David H. C. Du (F'98) received the B.S. degree in mathematics from National Tsing-Hua University, Taiwan, in 1974, and the M.S. and Ph.D. degrees in computer science from the University of Washington, Seattle, in 1980 and 1981, respectively. He is currently the Qwest Chair Professor with the Computer Science and Engineering Department, University of Minnesota, Minneapolis. His research interests include cyber security, sensor networks, multimedia computing, storage systems, and high-speed networking.